PNAS
www.pnas.org

Supplementary Information for

Kv2 potassium channels form endoplasmic reticulum/plasma membrane junctions via interaction withVAPA and VAPB

Ben Johnson[a,b], Ashley N. Leek[a,b], Laura Solé[a,b], Emily E. Maverick[a,b], Tim P. Levine[c], and Michael M. Tamkun[a,b,d]

[a]Department of Biomedical Sciences, Colorado State University, Fort Collins, CO 80523; [b]Program in Molecular, Cellular, and Integrative Neurosciences, Colorado State University, Fort Collins, CO 80523; [c]University College London Institute of Ophthalmology, London EC1V 9EL, United Kingdom; and [d]Department of Biochemistry and Molecular Biology, Colorado State University, Fort Collins, CO 80523

Michael M. Tamkun
Email: michael.tamkun@colostate.edu

This PDF file includes:

Supplementary text
Figs. S1 to S2
References for SI reference citations

www.pnas.org/cgi/doi/10.1073/pnas.1805757115

Supplementary Materials and Methods

DNA Constructs VAPA-GFP and VAPA(K87D/M89D)-GFP were provided by Axel Brunger via Addgene (Addgene plasmids 18874 and 18875, respectively). GFP-VAPB (1) was obtained from the DNASU Plasmid Repository. From these initial constructs, VAPB-GFP, VAPB-mRuby2, VAPB-Clover, and VAPA-paGFP were created using standard DNA manipulation techniques.

For the proximity biotinylation experiments AMIGO-YFP-APEX was generated from the APEX2-NES vector obtained from Alice Ting (Addgene plasmid # 49386). Overlap PCR was used to insert an EcoRI cut site (5'GACGGAGAATTCAAGGGATGGACTACAAGGATGAC3') in the APEX2-NES vector at the 5' end of APEX2 allowing the resulting XbaI and EcoRI APEX DNA to be added to the 3' end of AMIGO-YFP to form AMIGO-YFP-APEX.

pcDNA3.1-Clover-mRuby2 was a gift from Kurt Beam (Addgene plasmid # 49089), mRuby2-C1 was from Michael Davidson (Addgene plasmid # 54768) and pcDNA3-Clover was from Michael Lin (Addgene plasmid # 40259). An mClover-C1 construct was generated by digesting pcDNA3-Clover and mRuby2-C1 with NdeI and BsrGI and exchanging Ruby2 with Clover. Ruby2-Kv2.1 was generated from mRuby2-C1 and the previously described GFP-Kv2.1 (2) by replacing the NheI to EcoRI GFP encoding fragment in GFP-Kv2.1 with mRuby2. Clover-Kv2.1 was generated from mClover-C1 and a Ruby2-Kv2.1 by inserting the XhoI to XmaI fragment containing Kv2.1 into mClover-C1.

Generation of the CD4-based chimeras relied heavily on synthetic DNA obtained from Genewiz. CD4-Kv2.1:445-609 was created using synthetic DNA (amino acids 445-609 of Kv2.1) which were appended to wildtype CD4 using SacII and NotI restriction sites. The CD4-Kv2.2:452-911 was made using the same approach. In both of these constructs the VAP binding motif was the same distance from the CD4 transmembrane domain. The other CD4-Kv2.1 minimal FFAT sequence constructs (see Fig. 7) were based on work done in the Bjorkman laboratory (3), where the CD4 transmembrane domain was separated from the Kv2.1 channel sequence by using a combination of $(Gly_4Ser)_n$ linkers, to confer flexibility, with β2-microglobulin sequence to provide a more rigid structure. β2-microglobulin is a monomeric 12 kD protein with an N- to C-termini separation distance of ~3.5 nanometers (4). The Gly_4Ser linkers were of variable length so as to keep the total amino acid number from the CD4 transmembrane domain to the Kv2.1 FFAT motif consistent between the CD4-chimeric constructs and wildtype Kv2.1. For the oxysterol-binding protein (OSBP) FFAT motif (5) and flanker construct (CD4-OSBP(FFAT)), a single serine in the OSBP FFAT flanker region was changed to aspartic acid to *a priori* nullify any possible phosphorylation effects on VAP binding. All synthetic DNA segments were inserted into the CD4 backbone using SacII and XbaI restriction sites. All constructs

terminated in a stop codon inserted into the sequence immediately after the last amino acid of interest.

The luminal ER marker dsRedER has been previously described (6, 7). mCherry-JPH4 was provided by Yousang Gwack (Addgene 79599).

Microscopy Laser scanning confocal microscopy was performed using an Olympus FluoView 1000 inverted microscope equipped with two spectral detectors and one filter based detector in addition to an Ar laser (458/488/515 nm), 543 nm and 633 nm HeNe lasers and a 60X PlanApo, 1.4 NA, objective. Spinning disk confocal microscopy was performed using a Yokogawa-based CSUX1 system built around an Olympus IX83 inverted stand coupled to an Andor laser launch containing 405, 488, 561, and 637 nm diode lasers, 100-150 mW each. Images were collected using an Andor iXon EMCCD camera (DU-897) and 100X Plan Apo, 1.4 NA objective. This system is equipped with the ZDC constant focus system and a Tokai Hit chamber and objective heater. Unless stated otherwise, all images were acquired taken via spinning disk microscopy. When indicated, TIRF microscopy was performed on a Nikon Eclipse Ti fluorescence microscope with 405, 488, 561, and 633 nm diode lasers, 100 mW each, split evenly between TIRF and photoactivation unit pathways. However, 405 nm based activation of the photoactivatable GFP-VAPA presented in Fig. 5 was performed in TIRF to limit the activated GFP fluorescent to within 100 nm of the plasma membrane. TIRF images were collected using an Andor iXon EMCCD DU-897 camera through a Plan Apo 100x, NA 1.49, TIRF objective. Both the objective and dish are temperature controlled and z-drift was mitigated through the use of the Nikon Perfect-Focus system. With all three systems the appropriate use of spectral detectors, sequential excitation, dichroics and bandpass filters permitted fluorophore separation. Additional details regarding our microscopy have been previously described (6, 8, 9).

Supplementary figures

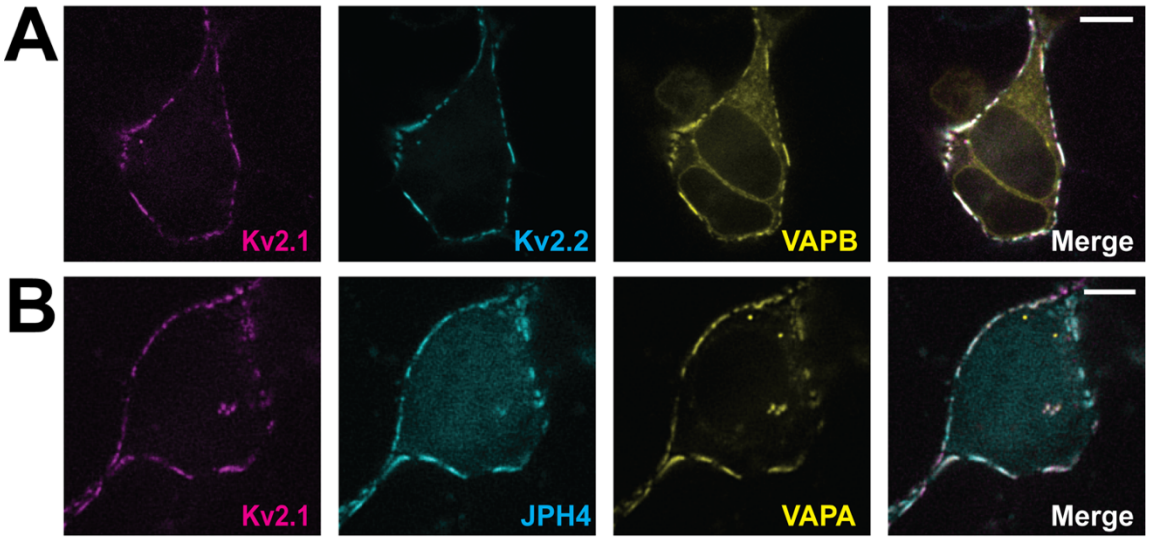

Fig. S1. The presence of Kv2.2 and junctophilin-4 do not alter the concentration of VAPs at Kv2.1- induced ER/PM contact sites. (A) Co-expression of Kv2.1-loopBAD labeled with streptavidin-CF640, GFP-Kv2.2, and mRuby2-VAPB. (B) Co-expression of Kv2.1-loopBAD labeled with streptavidin-CF640, mCherry-JPH4, and VAPA-GFP. Scale bars represent 10 μm.

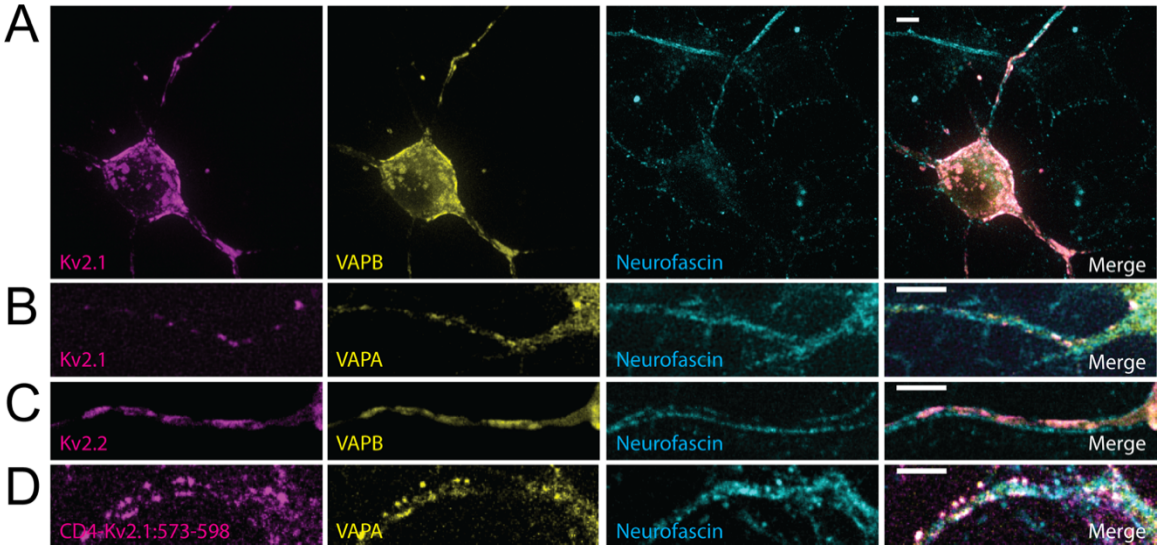

Fig. S2. Use of neurofascin immunostaining to identify the axon initial segment. (A) Representative image showing the localization of transfected Kv2.1-loopBAD, VAPB-GFP and neurofascin immuno-staining in live DIV 7 rat hippocampal neurons. Surface Kv2.1-loopBAD was visualized with CF640-conjugated streptavidin and antibody binding to extracellular neurofascin was detected using Alexa 594-conjugated goat anti-mouse secondary antibody. Note that the neurofascin-positive axon initial segment (AIS) in the top left corner is derived from a non-transfected neuron. (B) Colocalization of VAPA-GFP with Kv2.1 within the neurofascin-positive AIS. (C) Colocalization of VAPB-mRuby2 with GFP-Kv2.2 within the neurofascin-positive AIS (labeled with Alexa-647 secondary antibody). (D) Colocalization of VAPA-GFP with the CD4-Kv2.1:573-598 chimera (labeled with CF640-conjugated anti-CD4 antibody) within the neurofascin-positive AIS (labeled with the Alexa 594). All images are maximum intensity projections. Scale bars represent 5 μm.

References

1. Suzuki H*, et al.* (2009) ALS-linked P56S-VAPB, an aggregated loss-of-function mutant of VAPB, predisposes motor neurons to ER stress-related death by inducing aggregation of co-expressed wild-type VAPB. *J Neurochem.* 108(4):973-985.
2. O'Connell KM & Tamkun MM (2005) Targeting of voltage-gated potassium channel isoforms to distinct cell surface microdomains. *J Cell Sci* 118(Pt 10):2155-2166.
3. Klein JS, Jiang S, Galimidi RP, Keeffe JR, & Bjorkman PJ (2014) Design and characterization of structured protein linkers with differing flexibilities. *Protein Eng Des Sel.* 27(10):325-330.
4. Becker JW & Reeke GN, Jr. (1985) Three-dimensional structure of beta 2-microglobulin. *Proc Natl Acad Sci U S A.* 82(12):4225-4229.
5. Murphy SE & Levine TP (2016) VAP, a Versatile Access Point for the Endoplasmic Reticulum: Review and analysis of FFAT-like motifs in the VAPome. *Biochim Biophys Acta.* 1861(8 Pt B):952-961.
6. Fox PD*, et al.* (2015) Induction of stable ER-plasma-membrane junctions by Kv2.1 potassium channels. *J Cell Sci.* 128(11):2096-2105.
7. Fox PD*, et al.* (2013) Plasma membrane domains enriched in cortical endoplasmic reticulum function as membrane protein trafficking hubs. *Mol Biol Cell.* 24(17):2703-2713.
8. Akin EJ, Sole L, Dib-Hajj SD, Waxman SG, & Tamkun MM (2015) Preferential targeting of Nav1.6 voltage-gated Na^+ Channels to the axon initial segment during development. *PLoS One.* 10(4):e0124397.
9. Akin EJ*, et al.* (2016) Single-Molecule Imaging of Nav1.6 on the Surface of Hippocampal Neurons Reveals Somatic Nanoclusters. *Biophys J.* 111(6):1235-1247.